Received: 28 June 2017 | Accepted: 29 June 2017

DOI: 10.1002/hon.2466

WILEY

LETTER TO THE EDITOR

Microenvironment modulation and enhancement of antilymphoma therapy by the heparanase inhibitor roneparstat

To the Editor

The standard management of diffuse large B-cell lymphoma (DLBCL) relies on the chemotherapy combination including cyclophosphamide, doxorubicin, vincristine, and prednisone (CHOP). Although the introduction of anti-CD20 monoclonal antibody rituximab with CHOP chemotherapy has demonstrated a dramatic improvement in clinical outcome in CD20 positive patients,[1] most of them still face disease relapse. Thus, the challenge still remains to find more effective therapeutic approaches. The role of tumor microenvironment in modulating the drug sensitivity is increasingly becoming a key consideration for the development of novel anticancer agents. The endoglycosidase heparanase, through the cleavage of the heparan sulfate chains of heparan sulfate proteoglycans, partecipates in degradation and remodeling of the extracellular matrix (ECM) and promotes the functions of several bioactive molecules.[2] Clinically, heparanase is expressed at high levels in various malignancies and positively associated with progression and unfavorable prognosis.[3] Notably, recent advances have indicated a relevant role for heparanase in angiogenesis, metastasis, inflammation,[3-5] and lymphoma growth,[6,7] thus suggesting the endoglycosidase as a promising target for the development of innovative anticancer therapy. Here, using the SUDHL-4 as a preclinical model of aggressive DLBCL poorly responsive to single-agent conventional therapies[8] and expressing heparanase (Figure 1A i left), we report the effects induced by the heparanase inhibitor roneparstat, an heparan sulfate mimic glycol-split heparin,[9] in combination with clinically available agents.

Although roneparstat alone induced an early tumor growth inhibition rapidly resolved in tumor re-growth, as indicated by the low log cell kill (LCK) values (Table 1), the addition of the heparanase inhibitor could overcome the poor susceptibility of SUDHL-4 xenografts to dexamethasone and cyclophosphamide. Indeed, the combination resulted in a strongly enhanced tumor growth inhibition, supported by improvement in LCK values compared with single agent therapies (Figure 1A ii-iii, Table 1). In agreement with the high CD20 levels (Figure 1A i), SUDHL-4 tumors displayed a relevant sensitivity to rituximab, with 1 out of 6 treated mice experiencing complete response. Strikingly, the combination of roneparstat with rituximab produced the most impressive response, characterized by a remarkable increase in LCK value, complete regression in 5 out of 6 treated mice, and no evidence of disease in 3 out of 6 mice at 80 days after treatment interruption (Figure 1A iv, Table 1).

Histological analyses of tumors revealed the lack of a direct citotoxicity of roneparstat on lymphoma cells, rather inflammatory cell infiltration and fibro-vascular stroma disarrangement (Figure 1B i-ii), whereas a significant increase in cytotoxic effect ($P < 0.05$) (Figure 1C i) associated to a pronounced monocytoid and granulocytic myeloid cell infiltration was detected in rituximab-treated tumors (Figure 1B i). Notably, combination-treated tumors displayed a significantly higher number of apoptotic/necrotic cells compared to single treatment ($P < 0.0001$) (Figure 1C i) associated to a conspicuous inflammatory cell infiltration and an impaired stromal scaffolding as evidenced by an altered and incomplete reticulin fiber network (Figure 1B i-ii). Because of the deep stromal alteration induced by the combination treatment, we investigated as a possible mechanism through which roneparstat coud have positively modulated the tumor sensitivity to rituximab, the recruitment of complement components, the first murine component of the classical pathway C1q, and the activation factor C5. The in situ analyses showed a positive staining for C1q factor located near stromal elements in rituximab- and in combination-treated tumors, whereas it appeared confined to scattered infiltrating histiocytic cells in untreated and roneparstat-treated tumors (Figure 1B iii). Consistently, positive C5 staining was detected on the surface of lymphomatous and stromal elements in rituximab-treated and, more conspicuously, in combination-treated tumors, whereas it was restricted to few infiltrating myeloid elements in untreated and roneparstat-treated tumors (Figure 1B iv, Figure 1C ii).

To sum up, our present findings provide preclinical evidence that targeting the tumor microenvironment by roneparstat may enhance the antitumor activity of approved therapies for aggressive lymphomas with particular references to rituximab. These findings have clinical implications considering that roneparstat has completed phase I clinical trial in patients with multiple myeloma and early reports indicated a good tolerability.[10]

AUTHOR CONTRIBUTION

Conception and design of the study were done by FZ, MDN; acquisition of data was done by AR, GR, MDC, DC, MT, AG; analysis and interpretation of data were done by AR, CL, GC, RZ, CT; manuscript writing and review were done by AR, FZ, GC, CL, NZ, MDN.

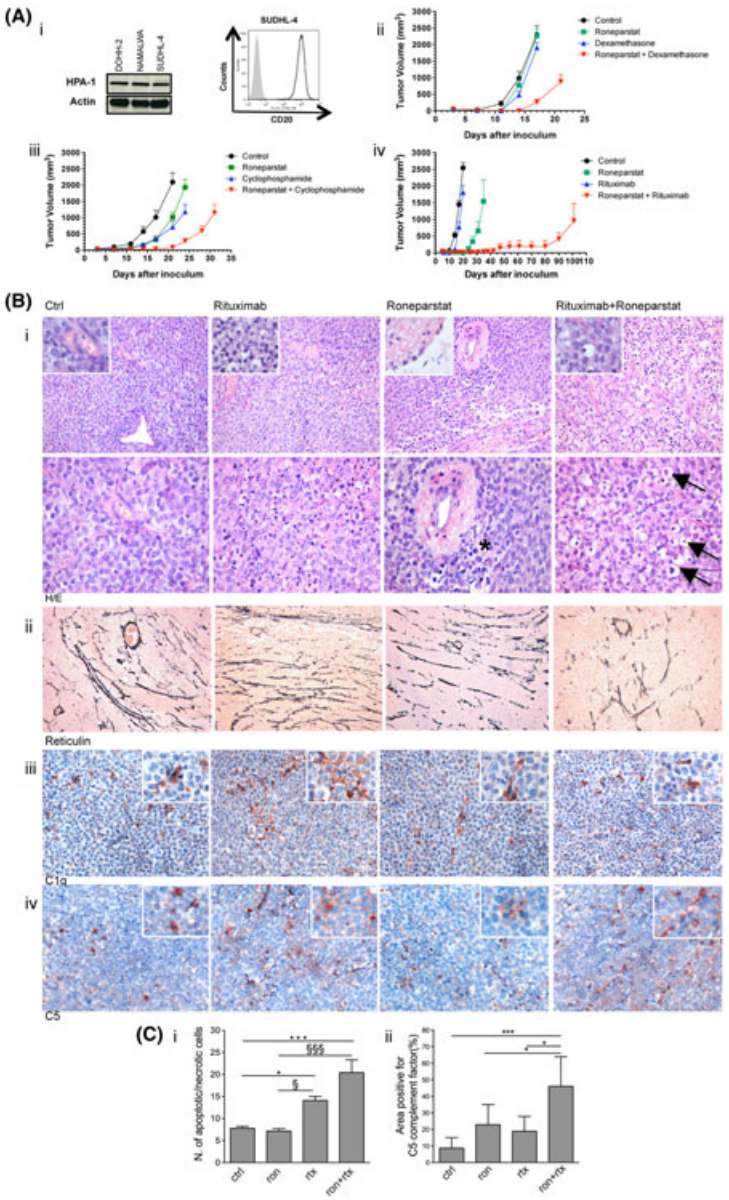

FIGURE 1 Antitumor activity of roneparstat in combination with antilymphoma agents and effects on tumor and stroma of SUDHL-4 xenografts. **A** (i) Western blot analysis revealed similar expression levels of heparanase (HPA-1) in the indicated B-NHL cell lines; β-actin was used as loading control. Cropped images are shown (*left panel*). Flow cytometric analysis of CD20 in the SUDHL-4 cell line. Histograms of anti-CD20 stained samples (open) and isotype control-stained samples (shaded) are representative of 3 independent analyses (*right panel*). Antitumor activity of roneparstat alone and in combination with (ii) dexamethasone or (iii) cyclophosphamide or (iv) rituximab in SCID mice (5-7 animals/group) injected s.c. with SUDHL-4 tumor fragments. Drug treatment started when tumor volume was around 50 mm^3. Roneparstat was administered s.c. (60 mg/kg/injection) twice a day for 5 d/wk for 3 wk in (ii) and (iv) and for 4 wk in (iii). Dexamethasone was administered i.p. (2 mg/kg) daily for 5 d/wk for 3 wk; cyclophosphamide was injected i.v. (50 mg/kg) every 7 d for 3 times; rituximab was given i.p. (5 mg/kg) every 3-4 d, for 6 times. Control mice were treated with vehicle alone. Tumor volumes were measured twice a week and reported as mean tumor volume ± S.E.M. **B** Histological/immunohistochemical analyses on tumors (300-400 mm^3) explanted after 4 d of treatment with roneparstat and/or rituximab (3-4 animals/group). (i) Representative microphotographs of tumor sections stained with hematoxylin and eosin. Rituximab-treated tumors displayed a remarkable presence of apoptotic/necrotic cells (inset); inflammatory cell infiltration and signs of fibro-vascular stroma disarrangement (asterisk) characterized roneparstat-treated tumors; combination therapy-treated tumors showed several cells with apoptotic nuclei (arrows) and a marked impairment of stromal architecture (original magnification ×20 up, ×40 down, inset ×63). (ii) Representative images of stromal reticulin network visualized with Gomori silver staining. Reticulin deposition was evidenced in the form of black/gray stripes. (original magnification ×20). (iii) Representative microphotographs showing the immunohistochemical detection of the first murine complement factor C1q and (iv) the complement activation factor C5 (original magnification ×20; inset ×63). Immunostaining was revealed by polymer detection kit and AEC (3-amino-9-ethylcarbazole) substrate chromogen. The slides were counterstained with Harris hematoxylin. **C** Quantitative analysis of apoptotic/necrotic figures (i) in tumor sections from mice treated with roneparstat (ron), rituximab (rtx), roneparstat plus rituximab and untreated control mice (ctrl). For each sample, the number of apoptotic/necrotic cells was counted in 10 randomly selected microscopic fields (40×). For quantification of C5 complement factor (ii), 5 pictures/sample at 4× magnification were captured covering the vast majority of the sample, and analyzed using image analysis software. Data are reported as mean ± S.D.; § $P < 0.05$, §§§ $P < 0.0001$ by ANOVA; post hoc tests by Bonferroni's multiple comparison test. *$P < 0.05$, ***$P < 0.0001$ by ANOVA; post hoc test by Dunnet's multiple comparison test

TABLE 1 Antitumor effects of roneparstat in combination with clinical agents against human SUDHL-4 xenografts

Drug	Dose (mg/kg)	Schedule	MaxTVI%[a] (day)	TVI(%)[b] (day)	CR[c]	NED[d]	LCK[e]
Roneparstat	60	2qdx5/wx3w	100(11)	2(17)	-	-	0.2
Dexamethasone	2	qdx5/wx3w	100(11)	17	-	-	0.4
Combination				89**	-	-	1.4
Roneparstat	60	2qdx5/wx4w	75(14)	52(21)	-	-	0.5
Cyclophosphamide	50	q7dx3	70(14)	66	-	-	0.5
Combination				96**	-	-	1.4
Roneparstat	60	2qdx5/wx3w	75(14)	29(20)	-	-	0.5
Rituximab	5	q3-4dx6	99(20)	99	1/6	-	2.5
Combination				99	5/6*	3/6	12.5

All treatments were well tolerated.

[a]Highest value of tumor volume inhibition percentage (TVI %) achieved by single-agent treatment; in parentheses, the day of evaluation.

[b]TVI% in treated over control mice; in parentheses the day of evaluation corresponding to the maximum inhibition by the combination (in most experiments at the end of treatment).

[c]CR, complete regression, ie, disappearance of the tumors lasting at least 10 d after the end of treatments.

[d]NED, mice with no evidence of disease at the end of the experiment.

[e]LCK, Log10 cell kill to reach 500 mm^3 of tumor volume.

**$P < 0.01$ by Student's test vs single drug-treated mice.

*$P < 0.05$ by Fisher's exact test vs single drug-treated mice.

CONFLICT OF INTEREST

Roneparstat is a proprietary drug of Leadiant Biosciences SA (formerly sigma-tau Research Switzerland SA). Zunino F and Zaffaroni N received grant support from Leadiant Biosciences SA. No potential conflicts of interest were disclosed by the other authors.

Anna Rossini[1]
Franco Zunino[2]
Giusi Ruggiero[1]
Michelandrea De Cesare[2]
Denis Cominetti[2]
Monica Tortoreto[2]
Cinzia Lanzi[2]
Giuliana Cassinelli[2]
Roberta Zappasodi[1]
Claudio Tripodo[3]
Alessandro Gulino[3]
Nadia Zaffaroni[2]
Massimo Di Nicola[1]

[1]*Unit of Immunotherapy and Anticancer Innovative Therapeutics, Department of Medical Oncology, Fondazione IRCCS Istituto Nazionale dei Tumori, Milan, Italy*

[2]*Molecular Pharmacology Unit, Department of Applied Research and Technological Development, Fondazione IRCCS Istituto Nazionale dei Tumori, Milan, Italy*

[3]*Tumor Immunology Unit, Department of Health Science, Human Pathology Section, University of Palermo, School of Medicine, Palermo, Italy*

Correspondence
Massimo Di Nicola, Fondazione IRCCS Istituto Nazionale dei Tumori, Via G. Venezian 1, 20133 Milan, Italy.
Email: massimo.dinicola@istitutotumori.mi.it

REFERENCES

1. Cheson BD, Leonard JP. Monoclonal antibody therapy for B-cell non Hodgkin's lymphoma. *N Engl J Med*. 2008;359(6):613-626. https://doi.org/10.1056/NEJMra0708875
2. Chiodelli P, Bugatti A, Urbinati C, Rusnati M. Heparin/Heparan sulfate proteoglycans glycomic interactome in angiogenesis: biological implications and therapeutical use. *Molecules*. 2015;20(4):6342-6388. https://doi.org/10.3390/molecules20046342
3. Ilan N, Elkin M, Vlodsvsky I. Regulation, function and clinical significance of heparanase in cancer metastasis and angiogenesis. *Int J Biochem Cell Biol*. 2006;38(12):2018-2039. https://doi.org/10.1016/j.biocel.2006.06.004
4. Vlodavsky I, Beckhove P, Lerner I, et al. Significance of heparanase in cancer and inflammation. *Cancer Microenviron*. 2012;5(2):115-132. https://doi.org/10.1007/s12307-011-0082-7
5. Pisano C, Vlodavsky I, Ilan N, Zunino F. The potential of heparanase as a therapeutic target in cancer. *Biochem Pharmacol*. 2014;89(1):12-19. https://doi.org/10.1016/j.bcp.2014.02.010
6. Weissmann M, Arvatz G, Horowitz N, et al. Heparanase-neutralizing antibodies attenuate lymphoma tumor growth and metastasis. *PNAS*. 2016;113(3):704-709. https://doi.org/10.1073/pnas.1519453113
7. Brennan TV, Lin L, Brandstadter JD, et al. Heparan sulfate mimetic PG545-mediated antilymphoma effects require TLR9-dependent NK cell activation. *J Clin Invest*. 2016;126(1):207-219. https://doi.org/10.1172/JCI76566
8. Olejniczack SH, Hernandez-Ilizaliturri, Clemts JL, Czuczman MS. Acquired resistance to rituximab is associated with chemotherapy resistance resulting from decreased Bax and Bak expression. *Clin Cancer Res*. 2008;14(5):1550-1560. https://doi.org/10.1158/1078-0432.CCR-07-1255
9. Naggi A, Casu B, Perez M, *et al*. Modulation of the heparanase-inhibiting activity of heparin through selective desulfation, graded N-acetylation, and glycol splitting. *J Biol Chem* 2005;280(13):12103-12113. DOI: https://doi.org/10.1074/jbc.M414217200
10. Galli M, Magen H, Einsele H, et al. Roneparstat (SST0001), an innovative heparanase (HPSE) inhibitor for multiple myeloma (MM) therapy: first in man study. *Blood*. 2015;126(23):3246 (abstract)